Low-Flow Piezoelectric Mist Cooling of an Automotive Radiator: An Experimental Study

Lim Kian Kiat[1], Ting Tiew Wei[1,2,*], Thomas Moh Shan Yau[1]

[1]School of Engineering and Technology, University of Technology Sarawak, 96000 Sibu, Sarawak, Malaysia

[2]Centre for Research of Innovation and Sustainable Development, University of Technology Sarawak, 96000 Sibu, Sarawak, Malaysia

***Corresponding Author**

DOI: https://doi.org/10.51584/IJRIAS.2026.11100105

Received: 28 October 2026; Accepted: 02 November 2026; Published: 17 November 2026

ABSTRACT

Modern vehicles are more compact, and fuel cell vehicles (FCVs) are becoming more common. Both trends make radiator cooling harder. There is little space for a larger radiator or more air flow. FCVs produce water as a by-product, and this water could be used to cool the radiator. This study tests piezoelectric-actuated spray cooling on an automotive radiator. Two piezoelectric atomizers were placed in front of a flat-tube radiator with louvered fins. The radiator fan drew the water mist through the core. The coolant was water, in laminar flow (Reynolds number of about 195 to 270). The heating power was 2000, 2500 or 3500 W, which gave coolant inlet temperatures of 41.5 to 61.1 °C. The air velocity was 1.7, 2.0 or 2.3 m/s. The spray flow rate was 0, 5.56×10^{-8} or 1.28×10^{-7} m^3/s (3.3 to 7.7 mL/min). Performance was measured by an effective coolant-side Nusselt number. Its uncertainty was 13% to 28%. At the higher spray flow rate, the effective Nusselt number rose by 31.4% to 49.4% over the range of heating power. The enhancement did not rise steadily with heating power. The effect of the spray depended on air velocity. The enhancement was 6.2% at 1.7 m/s and 49.4% at 2.3 m/s. At 1.7 m/s, it was within the measurement uncertainty. From 1.7 to 2.3 m/s, the Nusselt number rose by a factor of 1.54 with the higher spray flow rate and 1.09 without spray. These results suggest that a low-flow piezoelectric spray can improve radiator heat transfer, mainly at higher air velocity. Further tests at engine coolant temperatures and higher coolant flow rates are needed.

Keywords: Spray cooling, Piezoelectric atomizer, Automotive radiator, Convective heat transfer, Heat transfer enhancement

INTRODUCTION

Engines are becoming more powerful, and vehicles are becoming more compact. This makes the cooling system more important. The radiator removes engine heat to the ambient air by convection. If it fails to do so, the engine can overheat. Engine efficiency, emissions and component life all depend on good heat management [1]. Many studies have improved radiator fins and tubes. Examples are new fin designs [2, 3] and micro-channels in the tubes [3]. However, the space for the radiator is shrinking. Engine overheating and the low thermal conductivity of the coolant limit how small a radiator can be [4]. Slotted fins on engine cylinders [5] and nanofluid coolants [4, 6] have also been studied. A compact engine bay also limits the air flow through the radiator. Radiator heat transfer falls as the air velocity falls [4].

Cooling is a particular issue in fuel cell vehicles (FCVs). Proton exchange membrane (PEM) fuel cells produce heat as well as water. They must work in a narrow temperature range, because the membrane can dry out or break down at high temperature [7]. At high load and high ambient temperature, the cooling system of a fuel cell truck may not remove all of this heat [8]. However, water is the only chemical product of a PEM fuel cell. This water could be used to cool the air side of the radiator.

Spray cooling is one way to do this. It breaks a liquid into fine droplets. When the droplets hit the hot surface, they remove heat by convection and by evaporation or boiling [9]. In a piezoelectric atomizer, an electric field makes the actuator vibrate at ultrasonic frequency. The vibration breaks the liquid into droplets [9]. The droplet size depends on the micropore diameter and on the vibration of the micropore plate [10].

Several studies have used piezoelectric sprays for cooling. Chen et al. [11] cooled a heated surface with a piezoelectric atomizer. A larger micropore diameter gave more uniform cooling. Soriano et al. [12] studied single and multiple droplet streams from a piezoelectric droplet generator. Flow rate, impingement frequency, droplet velocity and stream spacing all affected the heat transfer. Hsieh et al. [13] cooled a high-power LED with a piezoelectric microspray. Lu et al. [14] built a low-power micro spray system with a piezoelectric micro-dispenser to cool the inside of a car. Hsieh et al. [15] also studied a piezoelectric atomizer with a single-hole micronozzle. The spray height and the initial surface temperature affected the heat transfer.

Spray cooling has several advantages. It can remove high heat fluxes with a small amount of liquid [16]. The liquid film on the surface evaporates, so a lower wall superheat is needed [17]. Sprays can also cool a large surface evenly [16, 18]. Piezoelectric atomizers are small and use little water. These features suit the limited space under a vehicle hood.

Water mist is also used to pre-cool the air entering air-cooled heat exchangers. The fine droplets evaporate in the air stream and lower the air temperature before it reaches the fins. Martínez et al. [19] tested an ultrasonic mist generator as a pre-cooler for air-conditioner condensers. Such a generator causes no pressure loss in the air entering the condenser. Ahmed et al. [20] used an ultrasonic humidifier to pre-cool a home air-conditioner condenser. Together with an evaporative pad, it raised the average coefficient of performance by 35.4%. Bop and Dieng [21] sprayed only 0.0065 L/min of water ahead of a condenser, which cooled the inlet air from 32 to 27.4 °C. Water that does not evaporate can cause corrosion, so the amount of water must suit the air conditions [22].

Spraying water onto the radiator has also been studied for FCVs. These studies used the water produced by the fuel cell. Wagenblast et al. [8] designed a spray cooling system for a heavy-duty fuel cell truck. It collected water at low and medium load and sprayed it at high load. In simulations of two high-load driving cycles, the spray added cooling capacity to the conventional system. Su et al. [23] tested water spray on an FCV radiator, on a test bench and by simulation. An inclined spray was more effective than a vertical one. Park et al. [24] studied an evaporative cooling system for an FCV by simulation and testing. They studied the effects of the water mass flow rate, spray angle, nozzle position and pressure. Mohamed Souby et al. [25] sprayed fuel cell water onto a stack radiator through a nozzle. Heat rejection rose by 167.7%, but the air pressure drop rose by 124.1%. Zeng et al. [26] used air-assisted nozzles and found the best spray pressure, distance and angle.

These studies used spray nozzles [24–26]. The best spray flow rates were about 0.3 L/min [25] and 0.6 L/min [23]. The ultrasonic atomizers used here need no pump or pressure nozzle. They make a fine mist at a much lower flow rate, 3.3 to 7.7 mL/min. The radiator fan draws this mist through the core. We found no study of such a low-flow mist on an automotive radiator.

This study has two objectives. The first is to set up a low-flow piezoelectric mist cooling arrangement for an automotive radiator. The second is to compare the radiator's heat transfer with and without the spray. We varied the heating power, air velocity and spray flow rate. We then measured their effect on the coolant-side Nusselt number.

MATERIALS AND METHODS

Experimental setup

Figure 1 shows the test rig. The test radiator was taken from a Perodua Myvi (2005 model). Its core has vertical aluminum flat tubes with rounded ends. Thin louvered aluminum fins fill the space between the tubes. Figure 2 shows the dimensions of one flat tube.

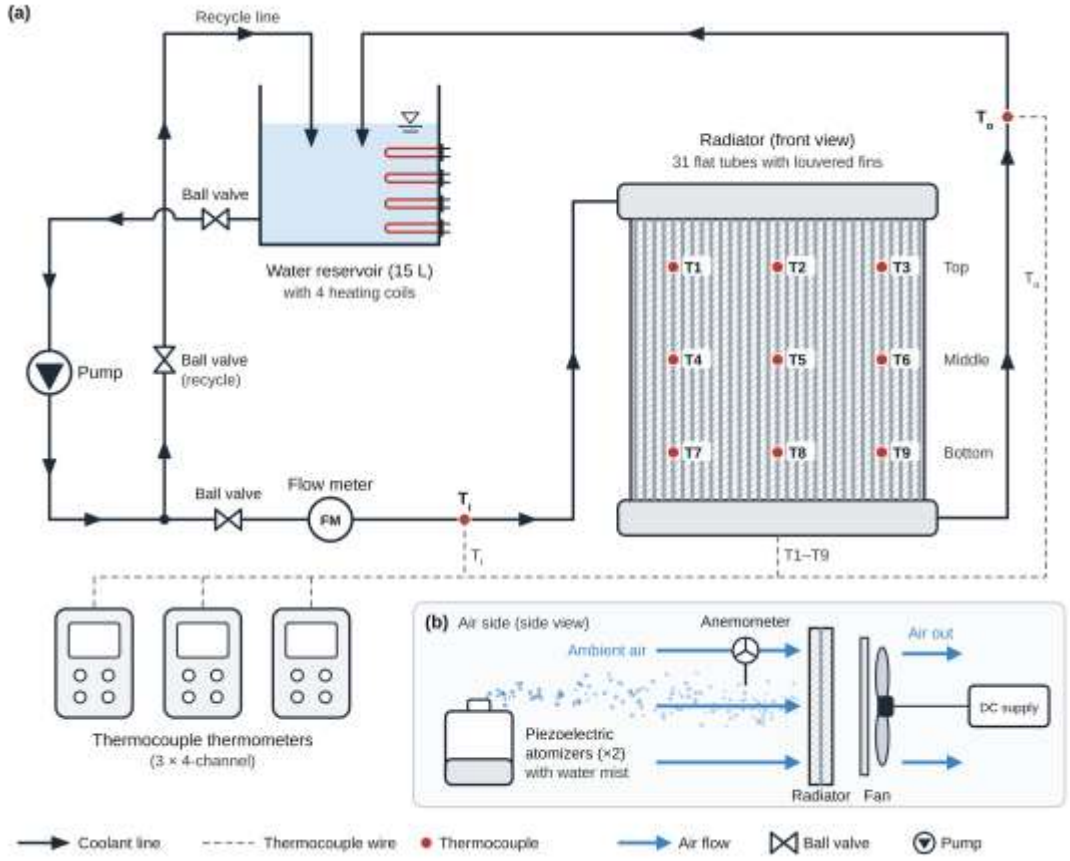


Figure 1: Schematic diagram of the experimental setup. (a) Coolant loop, with the inlet (T_i), outlet (T_o) and tube wall (T1 to T9) thermocouples. (b) Air side (side view), with the piezoelectric atomizers in front of the radiator and the fan behind it.

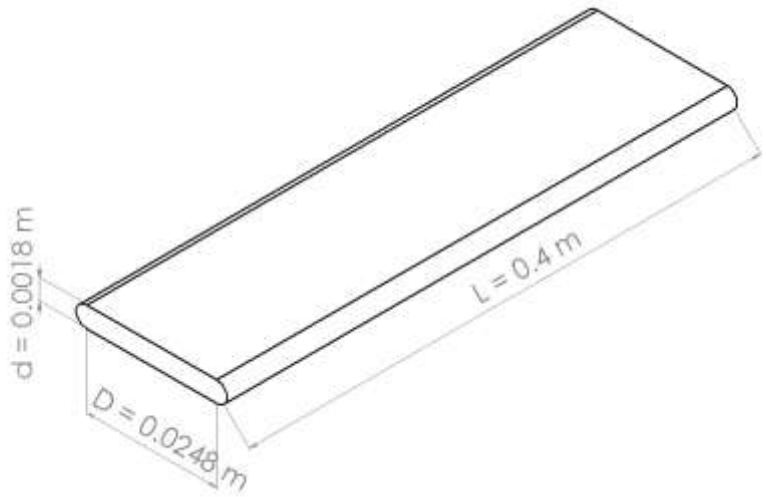


Figure 2: Dimensions of the radiator flat tube.

Water was used as the coolant. It was heated in a 15 L reservoir. The reservoir had two 2500 W and two 1000 W heating coils. These coils simulated the engine heat. They gave nominal heating powers of 2000, 2500 and 3500 W. Two 1000 W coils gave 2000 W. One 2500 W coil gave 2500 W. One 1000 W coil and one 2500 W coil together gave 3500 W. A pump circulated the coolant through the radiator. Three ball valves set the coolant flow rate. A flow meter measured it. The radiator fan was mounted behind the radiator. It drew ambient air across the core, so the air and coolant were in cross flow. The air velocity was set through the DC supply to the fan. A digital anemometer measured it in front of the core.

ISSN No. 2454-6194 | DOI: 10.51584/IJRIAS |Volume XI Issue X October 2026

Nine bare-wire thermocouples measured the tube wall temperature. Three were placed in each of the top, middle and bottom sections (T1 to T9 in Fig. 1a). Thermal paste improved the contact between the tube wall and each thermocouple. Two more thermocouples measured the coolant inlet and outlet temperatures. Three four-channel thermocouple thermometers recorded all readings.

The two spray units were commercial ultrasonic atomizers, each with its own water tank. Each unit atomizes water with a piezoelectric transducer that vibrates at ultrasonic frequency. The units were placed in front of the radiator, with their mist outlets facing the core (Fig. 1b). The radiator fan drew the mist through the core, so the spray acted on the air side. Each unit was run at two output levels, intermediate and maximum. The spray flow rate of each unit was found from the volume of water it used in a 3600 s run. Each unit was tested twice, and the mean was used. Together, the two units gave $Q_{spray} = 5.56 \times 10^{-8}$ m^3/s at the intermediate level and 1.28×10^{-7} m^3/s at the maximum level. These are 3.3 and 7.7 mL/min.

Test conditions

Table 1 lists the test conditions. Two test series were run. Each series was repeated at the three spray flow rates. The coolant flow rate was the same in all tests (Re ≈ 195 to 270). In the heating power series, P was 2000, 2500 or 3500 W, and the air velocity was 2.3 m/s. A higher heating power gave a higher coolant inlet temperature. The mean inlet temperature was 41.5 to 44.2 °C at 2000 W, 51.5 °C at 2500 W and 60.3 to 61.1 °C at 3500 W. In the air velocity series, V_{air} was 1.7, 2.0 or 2.3 m/s, and P = 2500 W. The coolant inlet temperature was 51.5 to 55.8 °C. The inlet temperature of a spray test and its no-spray reference differed by up to 2.2 K. The water properties were taken separately for each test. Both series share one operating point: P = 2500 W and V_{air} = 2.3 m/s. Each test ran until the temperature changed by less than 0.1 °C, which was taken as steady state. Each temperature was then read six times, and the mean was used.

Table 1: Operating conditions of the experiments.

Parameter	**Values**
Spray volumetric flow rate, Q_{spray} (m^3/s)	0; 5.56×10^{-8}; 1.28×10^{-7}
Coolant flow rate, flow meter reading (m^3/s)	5.00×10^{-5}
Coolant flow rate per tube, q (m^3/s)	1.61×10^{-6}
Coolant Reynolds number, Re	≈ 195 to 270 (laminar)
Nominal heating power, P (W)	2000; 2500; 3500
Air velocity, V_{air} (m/s)	1.7; 2.0; 2.3

Data reduction

The heat rejected by the coolant in one tube was found from the coolant energy balance [4]

$$Q = \dot{m}_c c_{p,c}(T_{c,i} - T_{c,o}) \quad (1)$$

where $\dot{m}$ is the mass flow rate, c_p is the specific heat, T_i and T_o are the inlet and outlet temperatures, and subscript "c" denotes the coolant. The coolant mass flow rate $\dot{m}_c$ can be defined as

$$\dot{m}_c = (\rho A_{cross} V)_c \quad (2)$$

where ρ is the coolant density, A_{cross} is the cross-sectional area and V is the coolant velocity. The volumetric flow rate q is expressed as

$$q = A_{\text{cross}} V \tag{3}$$

The coolant convective heat transfer coefficient can be determined by using [27]

$$h = \frac{Q}{A_{\text{surface}}(T_b - T_w)} \tag{4}$$

where $A_{surface}$ is the inner surface area of the radiator tube, T_b is the mean of the coolant inlet and outlet temperatures, and T_w is the mean of the nine tube wall temperatures (T1 to T9 in Fig. 1a). By using h, the Nusselt number can be expressed as [27]

$$\text{Nu} = \frac{hD_h}{k} \tag{5}$$

where D_h is the hydraulic diameter of the tube and k is the fluid thermal conductivity. The hydraulic diameter for a flat tube radiator can be calculated by using [28]

$$D_h = \frac{4\left[\frac{\pi}{4}d^2 + (D-d)d\right]}{\pi d + 2(D-d)} \tag{6}$$

For the present radiator, the major diameter of the flat tube is D = 0.0248 m. The minor diameter is d = 0.0018 m. The tube length is L = 0.4 m (Fig. 2). D and d were used as the inside dimensions of the tube. Equation (6) then gives D_h = 3.40 mm. The flow area of one tube is $A_{cross} = (\pi/4)d^2 + (D - d)d = 4.39 \times 10^{-5}$ m^2. The inner surface area of one tube is $A_{surface} = [\pi d + 2(D - d)]L = 0.0207$ m^2. The coolant-side equations are applied to one tube. The radiator has 31 tubes, so the flow rate per tube, q, is the flow meter reading divided by 31. This assumes equal flow in all tubes. The tube wall is thin aluminum, so the temperature drop across it was neglected. The water properties ρ, c_p, k and μ were taken at the coolant inlet temperature.

The coolant flow regime is described by the Reynolds number

$$\text{Re} = \frac{\rho V D_h}{\mu} \tag{7}$$

where ρ is the coolant density, V is the coolant velocity, D_h is the hydraulic diameter and μ is the dynamic viscosity of the coolant. The coolant velocity is found from the flow rate per tube, q:

$$V = \frac{q}{A_{\text{cross}}} \tag{8}$$

The coolant flow rate gives Re ≈ 195 to 270. This is below 2300, so the coolant flow was laminar in all tests [27].

The heat transfer enhancement compares the radiator with and without spray. Both cases use the same heating power, coolant flow rate and air velocity:

$$\text{E} = \frac{\text{Nu}_s - \text{Nu}_0}{\text{Nu}_0} \times 100\% \tag{9}$$

where Nu_s and Nu_0 are the Nusselt numbers with and without spray.

ISSN No. 2454-6194 | DOI: 10.51584/IJRIAS |Volume XI Issue X October 2026

Measurement uncertainty

The uncertainty in h, Nu and E was found by root-sum-square propagation. It combines the instrument accuracies in Table 2 and the scatter of the six readings. The thermocouple accuracy (±1 °C) was the main source. The uncertainty in Nu was 13% to 28%. Each spray test and its no-spray reference used the same sensors. Each thermocouple's fixed error was therefore taken to be the same in both tests, so it partly cancels in E. The instrument accuracy was treated as a limit, and the scatter of the six readings as a 95% confidence interval. The uncertainty in E was ±6 to ±15 percentage points. Table 3 lists the uncertainty of each result.

Table 2: Accuracy of the measuring instruments.

Instrument	**Accuracy**
Flow meter	± 2.68 × 10^{-7} m^3/s
Thermocouple	± 1 °C
Vernier caliper	± 0.01 mm

Table 3: Nusselt number, heat transfer enhancement and their uncertainties in all tests.

Test condition	**Q_{spray} (m^3/s)**	**Nu**	**Uncertainty in Nu (±%)**	**E (%)**	**Uncertainty in E (± points)**
2000 W, 2.3 m/s	0	2.358	28	–	–
	5.56 × 10^{-8}	2.670	25	13.2	15
	1.28 × 10^{-7}	3.099	28	31.4	12
2500 W, 2.3 m/s *	0	2.311	19	–	–
	5.56 × 10^{-8}	3.281	17	41.9	12
	1.28 × 10^{-7}	3.454	17	49.4	12
3500 W, 2.3 m/s	0	2.582	14	–	–
	5.56 × 10^{-8}	3.301	13	27.8	6
	1.28 × 10^{-7}	3.787	14	46.7	8
2500 W, 2.0 m/s	0	2.237	19	–	–
	5.56 × 10^{-8}	2.662	18	19.0	8
	1.28 × 10^{-7}	2.754	18	23.1	11
2500 W, 1.7 m/s	0	2.115	21	–	–
	5.56 × 10^{-8}	2.167	19	2.5	12
	1.28 × 10^{-7}	2.245	19	6.2	11

ISSN No. 2454-6194 | DOI: 10.51584/IJRIAS |Volume XI Issue X October 2026

Note: The test marked * is the shared operating point of the two test series. E was calculated from unrounded values of Nu.

RESULTS AND DISCUSSION

Here, h was found from the heat rejected and the difference between the mean coolant temperature and the measured wall temperature. When the air side improves, the measured heat rejection and the wall temperature change, so h changes too. Nu is therefore an effective value. It shows how much heat the radiator rejects for a given coolant-to-wall temperature difference. It is used here to compare tests.

Effect of heating power

Figure 3 shows the Nusselt number against heating power. The air velocity was 2.3 m/s. Without spray, Nu was 2.358 at 2000 W, 2.311 at 2500 W and 2.582 at 3500 W. These differences are smaller than the uncertainty in Nu. With spray, Nu was higher at every heating power. With $Q_{spray} = 1.28 \times 10^{-7}$ m^3/s, it was 3.099, 3.454 and 3.787. The value of 3.787 at 3500 W was the highest in this series. At each heating power, the higher spray flow rate gave the higher Nusselt number.

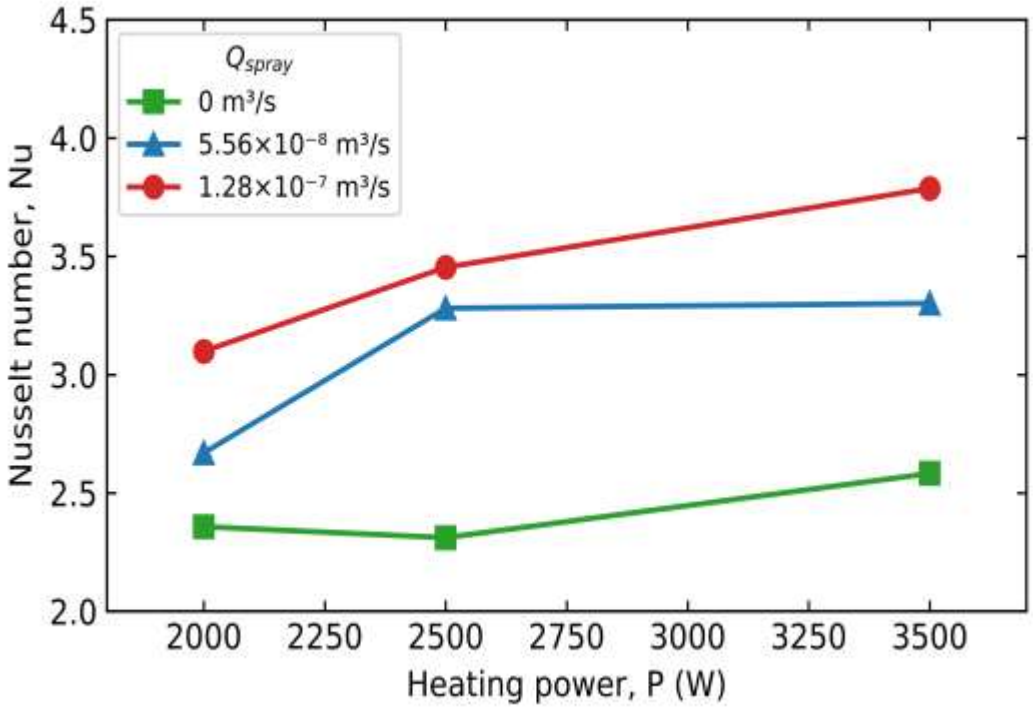


Figure 3: Nusselt number as a function of heating power for different spray volumetric flow rates (V_{air} = 2.3 m/s).

Figure 4 shows the enhancement defined in Eq. (9). With $Q_{spray} = 1.28 \times 10^{-7}$ m^3/s, the enhancement was 31.4% at 2000 W, 49.4% at 2500 W and 46.7% at 3500 W. With $Q_{spray} = 5.56 \times 10^{-8}$ m^3/s, it was 13.2%, 41.9% and 27.8%. The uncertainty in these values was ±6 to ±15 percentage points (Table 3). Only the value of 13.2% at 2000 W was within its uncertainty.

The enhancement was lowest at 2000 W at both spray flow rates. It did not rise steadily with heating power, because the values at 3500 W were not higher than those at 2500 W. The spray may help in two ways. Droplets that evaporate in the air cool it before it reaches the fins. Droplets that reach the fins wet them and evaporate there. These tests cannot separate the two, because the air temperature and droplet size were not measured.

ISSN No. 2454-6194 | DOI: 10.51584/IJRIAS |Volume XI Issue X October 2026

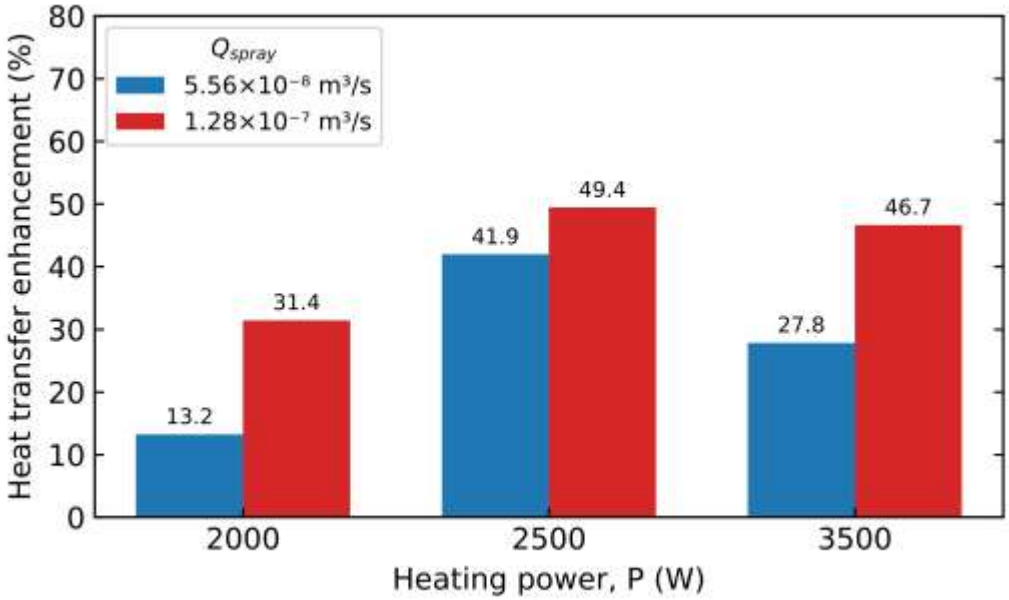


Figure 4: Heat transfer enhancement of piezoelectric-actuated spray cooling as a function of heating power (V_{air} = 2.3 m/s).

Effect of air velocity

The radiator fan draws ambient air through the fins. The fan's DC supply was used to set the air velocity. Figure 5 shows the Nusselt number against air velocity. The heating power was 2500 W. The coolant inlet temperature was 51.5 to 55.8 °C. The Nusselt number rose with air velocity at every spray flow rate. The highest value in this series was 3.454. It occurred at 2.3 m/s with $Q_{spray} = 1.28 \times 10^{-7}$ m^3/s. A higher air velocity raises the air-side heat transfer coefficient [27]. In these tests, the wall temperature fell and the measured heat rejection rose.

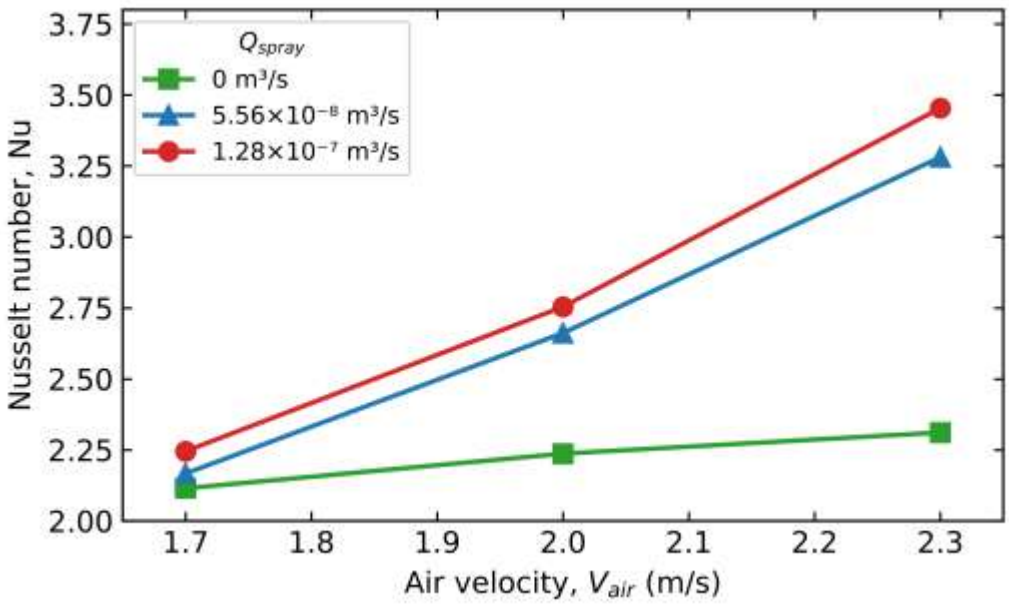


Figure 5: Nusselt number as a function of air velocity for different spray volumetric flow rates (P = 2500 W).

The spray flow rate changed the slope of these curves. From 1.7 to 2.3 m/s, Nu rose from 2.115 to 2.311 without spray. This is a factor of 1.09, which is within the uncertainty. With $Q_{spray} = 1.28 \times 10^{-7}$ m^3/s, Nu rose from 2.245 to 3.454. This is a factor of 1.54. The spray therefore had a larger effect at higher air velocity.

Figure 6 shows this as enhancement. With $Q_{spray} = 1.28 \times 10^{-7}$ m^3/s, the enhancement was 6.2% at 1.7 m/s, 23.1% at 2.0 m/s and 49.4% at 2.3 m/s. With $Q_{spray} = 5.56 \times 10^{-8}$ m^3/s, it was 2.5%, 19.0% and 41.9%. At 1.7 m/s, both values were within their uncertainty of ±11 to ±12 percentage points. At low fan speed, the spray therefore gave no clear benefit. A faster air stream may carry more droplets into the core. We did not measure the droplet flow, so this explanation is not confirmed.

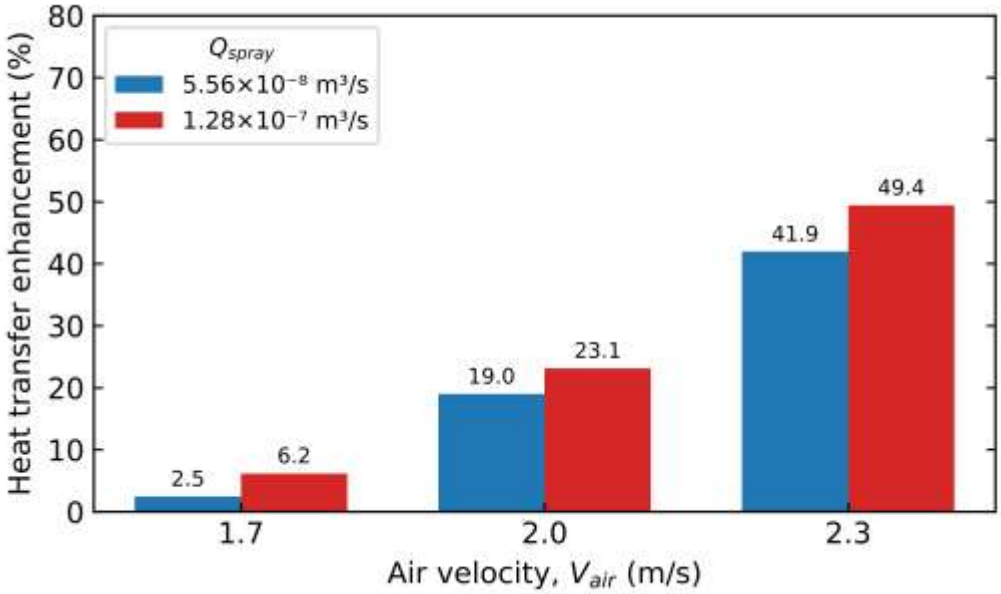


Figure 6: Heat transfer enhancement of piezoelectric-actuated spray cooling as a function of air velocity (P = 2500 W).

On the same rig, Huong et al. [4] also found that heat transfer rose with air velocity. The radiator sprays in [23] and [25] used far more water. Mohamed Souby et al. [25] raised heat rejection by 167.7% with 0.30 L/min, 40 to 90 times the flow used here, but the air pressure drop rose by 124.1%. These values are not directly comparable with the effective Nu used here. Bop and Dieng [21] found that a low-flow mist saturated the inlet air after 2 min of misting. At low air velocity, the same mist meets less air, which may explain the small benefit at 1.7 m/s. Humidity was not measured, so this is not confirmed.

Summary and limitations

Table 3 lists Nu and E for all 15 tests, with their uncertainties. The enhancement was larger than its uncertainty in 7 of the 10 spray tests. The three exceptions were the two tests at 1.7 m/s and the test at 2000 W with the lower spray flow rate. The highest enhancement was 49.4% ± 12 percentage points. It was found at the shared operating point with $Q_{spray} = 1.28 \times 10^{-7}$ m^3/s.

This study has limitations. The coolant inlet temperature was 41.5 to 61.1 °C. This is lower than in a typical engine cooling circuit. The coolant was water, not a water–glycol mixture. The thermocouples were accurate to ±1 °C. Tests were also run at two higher coolant flow rates, with flow meter readings of 18.33×10^{-5} and 41.67×10^{-5} m^3/s. There, the coolant temperature drop was only 0.95 to 3.65 K, and the uncertainty in Nu was 41% to 152%. Those tests are therefore not reported. Ambient air temperature and humidity were not recorded. Humidity limits how much water can evaporate, so it affects the spray. Each condition was run once, with six readings, so run-to-run repeatability was not measured. The coolant flow was assumed to be equal in all 31 tubes.

CONCLUSION

This study tested piezoelectric spray cooling on the air side of an automotive radiator. The heating power, air velocity and spray flow rate were varied, with laminar coolant flow. The spray raised the effective Nusselt

number by more than its uncertainty in 7 of 10 tests. With $Q_{spray} = 1.28 \times 10^{-7}$ m^3/s, the enhancement was 31.4% to 49.4% over the range of heating power. The enhancement did not rise steadily with heating power. It was lowest at 2000 W at both spray flow rates. The effect of the spray depended on air velocity. With $Q_{spray} = 1.28 \times 10^{-7}$ m^3/s, the enhancement was 6.2% at 1.7 m/s and 49.4% at 2.3 m/s. Over this range, Nu rose by a factor of 1.54 with spray and 1.09 without spray. These results suggest that piezoelectric spray cooling can improve radiator heat transfer, mainly at higher air velocity. It may suit FCVs, which produce water on board. Other vehicles would need a water tank. Future tests should use higher coolant temperatures, higher coolant flow rates and more accurate temperature sensors. The wall temperature also varied across the radiator (T1 to T9). Future work could direct the spray to selected regions of the core, such as near the inlet, middle or outlet.

REFERENCES

1. Abdullah, M., & Zoynal Abedin, M. (2024). Recent development of combined heat transfer performance for engine systems: A comprehensive review. Results in Surfaces and Interfaces, 15, 100212. https://doi.org/10.1016/j.rsurfi.2024.100212
2. Bhuiyan, A. A., & Islam, A. K. M. S. (2016). Thermal and hydraulic performance of finned-tube heat exchangers under different flow ranges: A review on modeling and experiment. International Journal of Heat and Mass Transfer, 101, 38–59. https://doi.org/10.1016/j.ijheatmasstransfer.2016.05.022
3. Singh, H., Ting, D. S.-K., Reader, G., Eshtiaghi, N., Ichiyanagi, M., & Suzuki, T. (2024). Experimental investigation of thermal performance of novel finned radiators for automotive cooling system. Journal of Thermal Science, 33(5), 1726–1743. https://doi.org/10.1007/s11630-024-1992-2
4. Huong, N. H., Ting, T. W., Toh, L. K. L., & Ngu, H. J. (2023). Experimental study on convective heat transfer enhancement of automotive radiator with graphene-nanoplatelet suspension. Journal of Advanced Research in Fluid Mechanics and Thermal Sciences, 101(2), 60–72. https://doi.org/10.37934/arfmts.101.2.6072
5. Muthuram, N., Kanchan, B. K., & Ajith Kumar, K. U. (2024). Improving engine cooling performance through slotted fin design: A steady-state thermal analysis study. Journal of Heat and Mass Transfer Research, 11(2), 211–224. https://doi.org/10.22075/JHMTR.2024.32559.1502
6. Toh, L. K. L., & Ting, T. W. (2024). Numerical simulation of graphene-nanoplatelet nanofluid convection in millimeter-sized automotive radiator. CFD Letters, 16(6), 32–52. https://doi.org/10.37934/cfdl.16.6.3252
7. Tawalbeh, M., Alarab, S., Al-Othman, A., & Javed, R. M. N. (2022). The operating parameters, structural composition, and fuel sustainability aspects of PEM fuel cells: A mini review. Fuels, 3(3), 449–474. https://doi.org/10.3390/fuels3030028
8. Wagenblast, M., Pollak, M., Trägner, J., Heinke, S., Tegethoff, W., Köhler, J., & Swoboda, J. (2022). Design and analysis of a spray cooling system for a heavy-duty fuel cell truck (SAE Technical Paper 2022-01-5054). SAE International. https://doi.org/10.4271/2022-01-5054
9. Ebadian, M. A., & Lin, C. X. (2011). A review of high-heat-flux heat removal technologies. Journal of Heat Transfer, 133(11), 110801. https://doi.org/10.1115/1.4004340
10. Kiyama, Y., Tominaga, Y., Kanda, T., Suzumori, K., Kishi, T., Yamada, Y., & Seno, N. (2012). Evaluation of generated micro droplets using micropore plates oscillated by ultrasonic torsional transducers. Sensors and Actuators A: Physical, 185, 92–100. https://doi.org/10.1016/j.sna.2012.08.007
11. Chen, H., Cheng, W.-L., Peng, Y.-H., Zhang, W.-W., & Jiang, L.-J. (2016). Experimental study on optimal spray parameters of piezoelectric atomizer based spray cooling. International Journal of Heat and Mass Transfer, 103, 57–65. https://doi.org/10.1016/j.ijheatmasstransfer.2016.07.037
12. Soriano, G. E., Zhang, T., & Alvarado, J. L. (2014). Study of the effects of single and multiple periodic droplet impingements on liquid film heat transfer. International Journal of Heat and Mass Transfer, 77, 449–463. https://doi.org/10.1016/j.ijheatmasstransfer.2014.04.075
13. Hsieh, S.-S., Hsu, Y.-F., & Wang, M.-L. (2014). A microspray-based cooling system for high powered LEDs. Energy Conversion and Management, 78, 338–346. https://doi.org/10.1016/j.enconman.2013.10.066

14. Lu, C.-F., Yang, J.-C., Chen, C.-J., & Fu, C.-C. (2010). Low power micro spray cooling system. In 2010 5th International Microsystems Packaging Assembly and Circuits Technology Conference (pp. 1–4). IEEE. https://doi.org/10.1109/IMPACT.2010.5699528
15. Hsieh, S.-S., Huang, C.-F., & Lu, Y.-M. (2020). Water spray heat transfer through a piezoelectric atomizer with a single-hole micronozzle. Journal of Mechanical Science and Technology, 34(8), 3427–3436. https://doi.org/10.1007/s12206-020-0735-x
16. Kim, J. (2007). Spray cooling heat transfer: The state of the art. International Journal of Heat and Fluid Flow, 28(4), 753–767. https://doi.org/10.1016/j.ijheatfluidflow.2006.09.003
17. Kandlikar, S. G., & Bapat, A. V. (2007). Evaluation of jet impingement, spray and microchannel chip cooling options for high heat flux removal. Heat Transfer Engineering, 28(11), 911–923. https://doi.org/10.1080/01457630701421703
18. Liang, G., & Mudawar, I. (2017). Review of spray cooling – Part 1: Single-phase and nucleate boiling regimes, and critical heat flux. International Journal of Heat and Mass Transfer, 115, 1174–1205. https://doi.org/10.1016/j.ijheatmasstransfer.2017.06.029
19. Martínez, P., Ruiz, J., Martín, Í., & Lucas, M. (2020). Experimental study of an ultrasonic mist generator as an evaporative cooler. Applied Thermal Engineering, 181, 116057. https://doi.org/10.1016/j.applthermaleng.2020.116057
20. Ahmed, F., Ramana, A. S., & Jayakumar, K. (2025). Experimental study on adiabatic pre-cooling systems for air cooled condensers in hot and humid climates. Scientific Reports, 15(1), 4933. https://doi.org/10.1038/s41598-024-82863-0
21. Bop, I., & Dieng, B. (2024). An experimental investigation on the role of the operating time of the mist device on the thermal performances of a water-sprayed air-cooled condenser and on the energy consumption of the cooling system. International Journal of Thermofluids, 24, 100956. https://doi.org/10.1016/j.ijft.2024.100956
22. Park, H., Roh, J., Oh, K. C., Cho, H., & Kim, J. (2022). Modeling and optimization of water mist system for effective air-cooled heat exchangers. International Journal of Heat and Mass Transfer, 184, 122297. https://doi.org/10.1016/j.ijheatmasstransfer.2021.122297
23. Su, C.-Q., Wang, S., Liu, X., Tao, Q., & Wang, Y.-P. (2022). Experimental and numerical investigation on spray cooling of radiator in fuel cell vehicle. Energy Reports, 8, 1283–1294. https://doi.org/10.1016/j.egyr.2021.11.174
24. Park, U. J., Kwon, S. B., Choi, K. J., Lee, G. W., & Oh, D. S. (2024). A preliminary study on the evaporative cooling system for FCEV (SAE Technical Paper 2024-01-2406). SAE International. https://doi.org/10.4271/2024-01-2406
25. Mohamed Souby, M., Prabakaran, R., & Kim, S. C. (2025). Nozzle spray-cooling coupled PEMFC stack radiator: Thermal-hydraulic performance and integrated correlations. Energy, 321, 135517. https://doi.org/10.1016/j.energy.2025.135517
26. Zeng, R., Kang, H., Umar, M., Liang, X., & Zhao, Y.-N. (2025). Design and thermal management study of fuel cell spray cooling system. Applied Thermal Engineering, 270, 126271. https://doi.org/10.1016/j.applthermaleng.2025.126271
27. Bergman, T. L., Lavine, A. S., Incropera, F. P., & DeWitt, D. P. (2017). Fundamentals of heat and mass transfer (8th ed.). Wiley.
28. Hussein, A. M., Bakar, R. A., & Kadirgama, K. (2014). Study of forced convection nanofluid heat transfer in the automotive cooling system. Case Studies in Thermal Engineering, 2, 50–61. https://doi.org/10.1016/j.csite.2013.12.001